

# Current status of ICRF system on EAST

C.M. Qin<sup>1)</sup>, Y.P. Zhao<sup>1)</sup>, X.J. Zhang<sup>1)</sup>, B.N. Wan<sup>1)</sup>, X.Z. Gong<sup>1)</sup>, Y.Z. Mao<sup>1)</sup>, S. Yuan<sup>1)</sup>, G. Chen<sup>1)</sup>, Y. Chen<sup>1)</sup>, L. Zhang<sup>1)</sup>, J.F. Chang<sup>1)</sup>, F.D. Wang<sup>1)</sup>, Y.M. Duan<sup>1)</sup>

<sup>1)</sup>Institute of Plasma Physics, Chinese Academy of Sciences, Hefei 230031, China

Email contact of main author: chmq@ipp.ac.cn

## Abstract

The ICRF heating system on EAST upgraded by active cooling aims for long pulse operation. In this paper, the main technical features of the ICRF system are described. One of a major challenges for long pulse operation is RF-edge interactions induced impurity production and heat loading. In EAST, ICRF antenna protections and Faraday screen bars damaged due to LH electron beam are found. Preliminary results for the analysis of the interaction between LHCD and ICRF antenna are discussed. Increase of metal impurities in the plasma during RF pulse and in a larger core radiation are also shown. These RF-edge interactions at EAST and some preliminary results for the optimizing RF performance will be presented.

**Keywords:** long pulse, ICRF, heat-load

**PACS:** 52.50.Qt, 52.55.Hc, 52.35.Bj

## INTRODUCTION

One of the research objectives of Experimental Advanced Superconducting Tokamak (EAST) is to perform a steady-state operation in a high performance regime [1]. Heating and current drive using fast wave in the Ion Cyclotron Range of Frequency (ICRF) have been proposed as one of the main tools for the advanced tokamak operation of EAST. The ICRF system on EAST has been developed for several years, which is upgraded by active cooling aims for long pulse operation with a frequency range of 25-70MHz. The ICRF system will deliver 12 MW(1.5MW×8 transmitter) of RF power to the plasma using two different ICRF antennas mounted in a mid-plane port[2]. The 2×2 loop antenna at B-port is fed at end and grounded at the other end. The 1×4 folded antenna at I-port is a fed at center and grounded at the other end. Both the current straps and Faraday shield of the two antennas are made of stainless steel and coated by B4C for mitigation high Z impurities.

## EXPERIMENTAL RESULTS

In EAST, all the transmission lines including liquid stub tuners are upgraded as active water cooling for long pulse operation. In order to remove the dissipated RF power and incoming plasma heat loads, the straps, Faraday shield and RF limiters also should be water cooled. The high voltage distribution region on the transmission line between antenna and liquid stub tuner is pressurized with 3 kg/cm<sup>2</sup> N<sub>2</sub> to minimize the arcing(Fig.1).

To guarantee that all the elements inside the EAST chamber are leak tight, they have to comply with an independent qualification tests before their installation on the tokamak. Especially, high pressure and high vacuum tests of water cooling circuits for the faraday screen were carried out. These tests are conducted on a vacuum test bed, capable of baking the two faradays to 200° C. The helium leak test at room temperature is made with the water cooling channel pressurized up to 60 bars, and to 40 bars at 200° C. The maximum allowed leak rate at 40 bars and T=200° C is 1×10<sup>-8</sup> Pam<sup>3</sup> s<sup>-1</sup>, while at 60 bars and T<60° C it is reduced to 1×10<sup>-10</sup> Pam<sup>3</sup>s<sup>-1</sup>. This procedure ensures that there is no water leak on components before their connection to the machine vacuum.

As the straps for the EAST ICRF antenna are closely packed, the phased current distribution at straps causes a power imbalance at each strap owing to the large mutual couplings between straps[3]. The RF matching are quite difficult due to the cross-talking between the current straps and power flows from one strap to the other, and often a high VSWR on the transmission line causes arcing. In order to mitigate the effect on the matching circuit, a resonant loop circuit decouples system is included. A schematic of the decouples system is illustrated in Fig. 2. A decouples circuit connected to each arm of the strap with an asymmetric feeding point accomplishes the out-of-phase condition at the strap feeding points. The total length of the top and bottom arms of the loop is a multiple wavelength, and the length difference is a half wavelength plus a multiple wavelength. The resonant loop feed points will be choice at

voltage maximum (purely real input impedance) to be independent of the resistive component of the antenna load. Fig.3 shows the decouplers distribution for I-port antenna and B-port antenna. in the case of I-port antenna, Five resonance loop circuits for I-port antenna and four resonance loop circuits for the  $2 \times 2$  straps B-port antenna were constructed by using available standard coaxial components. Therefore, in the ICRF program of 2014 EAST campaign, priority was given to the system reliability with the decouples. After installation of these nine resonant loop circuits, the admittance matrix was measured. By fine tuning at a frequency of 35 MHz, the decoupled forward scattering drops from -14dB to -50 dB at the frequency. Fig.4 shows the ICRF system reliable operation are achieved with injected RF power of 2.8MW. Fig.3b indicates that the  $2 \times 2$  straps B-port antenna and 4-straps I-port antenna work well by the adopting of nine decouples.

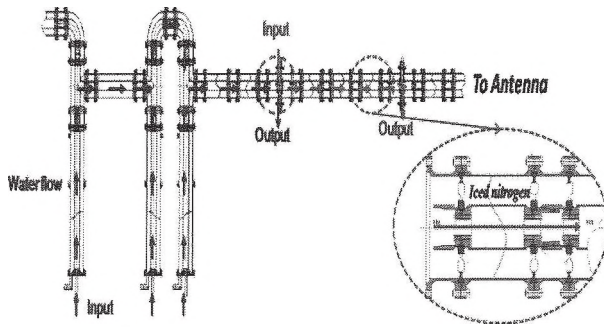


Figure1. Water cooling for matching system and transmission line with  $3 \text{ kg/cm}^2 \text{ N}_2$  for long pulse operation.

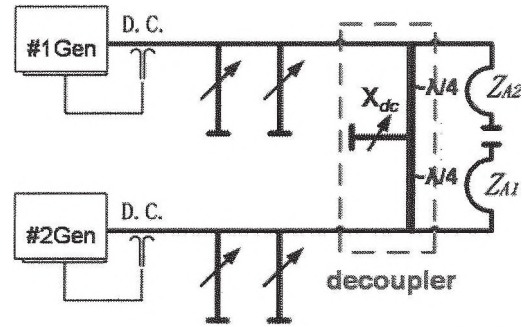


Figure2. A schematic of the decouples is included for two straps. The adopting of decouples cancels reactive mutual admittance by adjusting  $X_{dc}$ .

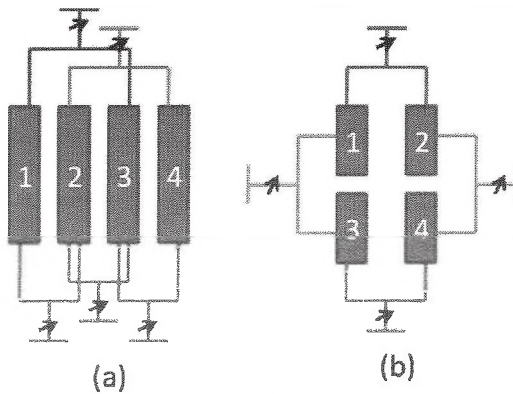


Figure3 Decouplers distribution for I-port antenna (a) and for B-port antenna (b).

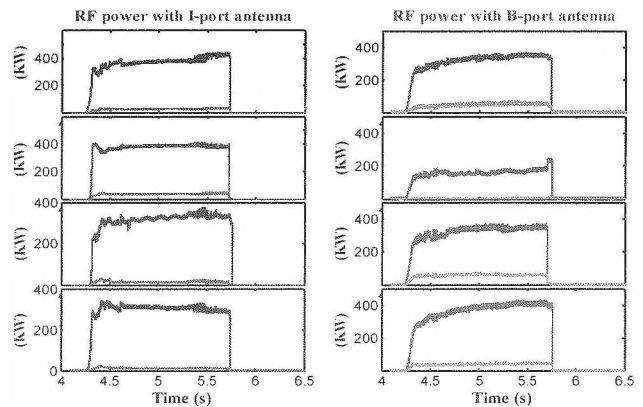


Figure 4. After installation of the decouplers, two antennas on EAST are reliable operation at 2.8MW power level with nine resonance loop circuits.

In the case of ICRF system stable operation, both ions and electrons heating were observed in the H-minority heating scheme in a deuterium majority plasma. An typical shot of ICRF heated discharge at  $B_t=2.5\text{T}$ ,  $I_p=500\text{kA}$  and  $H/(H+D)\sim 7\%$  is shown in Fig.5. The increase in the central ions and electrons temperature measured by X-ray crystal spectrometer were above 0.5keV during ICRF pulse. The stored energy has an increase of 15kJ and electron density drops by about 20%. Heating by ICRF waves may affect the underlying transport of particles in tokamak plasmas. Enhanced transport of particles may thus lead to reduced electron density.

One challenge to ICRF utilization for long pulse operation is its interaction with the edge plasma. A damage on the faraday screen bars of B-port antenna are observed. The most likely causes of the energetic electrons accelerated by launched LH waves, which follow magnetic field lines and thus intercept with ICRF antenna magnetic connection to LH grill waveguides. This phenomenon was observed previously on JET[4] and Tore Supra[5]. Fig.6a. shows a sketch of the field mapping between the LH Antenna and the LH launcher, both N-port LH and E-port LH antennas have some magnetic connections with B-port ICRF antenna. However, according to the direction of plasma, the electron side of the E-port LH antennas is consistent with the side of the melt FS(Fig.6b). As the RF limiters are located at the largest ripple of magnetic field and there is likely radial extension of the electron beam, so the FS is not protected by the RF limiter.

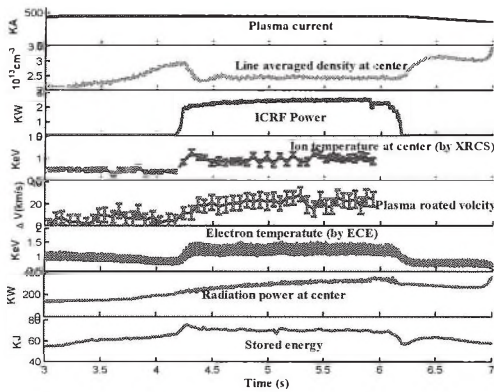


Figure 5. An example of typical ICRF Heating plasma discharge in EAST with 2.2MW of ICRF power injected show effective electron and ions heating.

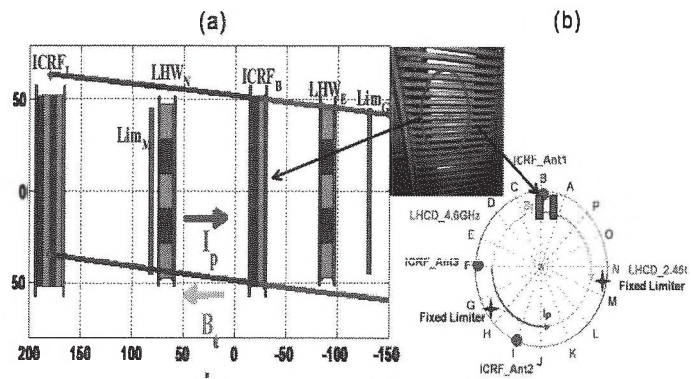


Figure 6. (a) A sketch of the magnetically connection between the LH Antenna and the LH launcher. (b) ICRF, LHCD and plasma limiter distribution on the top view of EAST. A damaged on the B-port Faraday screen bars E-port LH.

To monitor heat flux to the ICRF antenna, the antenna is instrumented with 5 thermocouples in the antenna each side protection tiles. Results from a statistical B-port and I-port side protection tiles measured by thermocouples, Fig.6 shows that the B-port antenna magnetic connection with LH powered receives significantly more heat flux. It suspects that fast electron beam production from E-port antenna and lead to more heat loads on the B-port antenna protect tiles. It is also found that warming up is very sensitive to LH pulse, the temperature increase greatly with long LH pulse. Without LH powered, B-port and I-port protection tiles have the similar temperature. #1 and #3 thermocouples responding to upper and middle region have much higher temperature than bottom protection tiles.

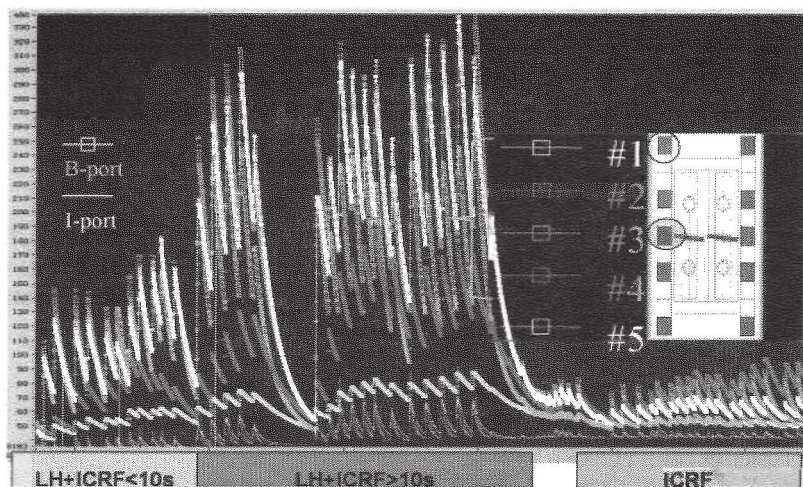


Figure 7. Temperature increase of protection limiter on the B-port and I-port. solid line with square maker is B-port temperature and solid line is I-port antenna. The square line is B-port ICRF antenna left limiter temperature measured by thermocouples, and solid line is I-port antenna left limiter temperature.

Release of metal impurities during ICRF pulse is often observed in many devices, especially in high Z metal Plasma Facing Components (PFCs) machine[AUG, JET, C-Mod]. EAST PFCs has been upgraded with tungsten upper divertor, molybdenum (Mo) first wall and C lower divertor since 2014 campaign. Signals from both, the bolometer and the UV spectrometer, Carbon and Mo, Fe and Cu impurities increase when the applying of ICRF power(see Fig8 ). However the intensity of Mo, Fe and Cu are more weaker than the intensity of CVI and N light impurities(Fig.9), and W line emission spectroscopy did not found during RF pulse. The intensity of CVI significantly enhancement is likely related to RF-sheaths due to lower divertor magnetic connection with active

